

Chapter

Introduction to MR spectroscopy in vivo

Key points

- Magnetic resonance spectroscopy (MRS) is an analytical technique widely used in chemistry for determining the structure of compounds, and the composition of mixtures of compounds.
- MRS is an insensitive technique, because it observes the resonance signal resulting from the tiny nuclear magnetization.
- Compounds are identified by their unique spectra, based on chemical shifts and coupling constants.
- Spectra are recorded using the pulsed Fourier transform technique.
- Proton spectroscopy of the human brain is most widely used, but other organ systems (such as breast, prostate) and nuclei (particularly ^{31}P and ^{13}C) have also been studied.
- In the brain, compounds of key importance measured by MRS include *N*-acetyl aspartate (located predominantly in neurons), choline, *myo*-inositol (located predominantly in glial cells), creatine, lactate, glutamate and glutamine.

Introduction

Nuclear magnetic resonance spectroscopy

The history of magnetic resonance spectroscopy (MRS) can be traced back to the first, independent observations of a nuclear magnetic resonance (NMR) signal in bulk matter by Bloch and Purcell in 1946.[1,2] When atomic nuclei which have the property of nuclear “spin” are placed in a static, strong magnetic field, their energy levels will vary depending on their orientation within the magnetic field. Due to the properties of quantum mechanics, only limited nuclear orientations are allowed (e.g. either “up” or “down” for spin-half nuclei such as the proton (^1H)). If an

oscillating radiofrequency field is then applied at the so-called “resonant frequency” corresponding to the energy difference between the different spin orientations, an absorption of power occurs which corresponds to spins being exchanged between the upper and lower states, and a radiofrequency signal is emitted by the sample. This resonant phenomenon and the resulting emitted radiofrequency signal is the fundamental principle of NMR, which is now used worldwide for both magnetic resonance imaging (MRI) and in vivo MRS.

Although NMR was originally a somewhat obscure technology of interest only to physicists for the measurement of gyromagnetic ratios (γ) of different nuclei (see below), applications of NMR to chemistry became apparent after the discovery of chemical shift and spin–spin coupling effects in 1950 and 1951, respectively.[3,4] These effects cause the resonant frequency of the NMR signal to change by small amounts (usually expressed in terms of parts per million (ppm) of the resonant frequency), because the local magnetic field surrounding each nucleus depends on both the structure of its surrounding electrons (i.e. the chemical structure of the molecule that the nuclei occur in) and also on the magnetic properties of neighboring nuclei. Thus, nuclei in different chemical environments will exhibit different resonant frequencies (or spectra in the case of molecules with multiple different nuclei), and NMR spectra can thereby be used to identify both the structure and relative concentrations of the molecules within the sample, information that can be of great value to chemists.

Major technical advances have occurred in MRS over the last several decades; two major developments in the 1960s included the introduction of superconducting magnets (1965), which were very stable and allowed higher field strengths than with conventional electromagnets to be attained, and in 1966 the use of the Fourier transform (FT) for signal processing. In nearly all contemporary spectrometers, the sample is subjected to periodic radiofrequency (RF) pulses

Chapter 1: Introduction to MR spectroscopy in vivo

directed perpendicular to the main magnetic field and the signal is Fourier transformed to give a spectrum in the frequency domain. FT NMR provides increased sensitivity compared to previous techniques, and also led to the development of a huge variety of pulsed NMR methods, including the methods now commonly used for MRI and in vivo MRS.

Basic theory

If the magnetic field is described by B_0 , then the energy of the nuclear spin state is given by

$$E = -\mu \cdot B_0 \quad (1.1)$$

where μ is the nuclear magnetic moment. The magnetic moment is related to the spin angular momentum, P , by the gyromagnetic ratio, γ ,

$$\mu = \gamma P = \gamma(I\hbar/2\pi) \quad (1.2)$$

where γ is a characteristic constant for each nucleus called the “gyromagnetic ratio”, I is the spin quantum number and \hbar is Planck’s constant (6.626068×10^{-34} J s). By definition, the direction of B_0 is taken to specify the Z-axis, so Equation (1.1) reduces to

$$E = -\mu_z B_0 \quad (1.3)$$

where μ_z is the component of μ along the Z-axis. For a nucleus with spin quantum number I , there are $(2I+1)$ different possible orientations of μ in the field, each with a component m_I in the Z direction. For example, for a spin 1/2 nucleus ($I = 1/2$), m_I can take the values $+1/2$ and $-1/2$ (Figure 1.1).

Applying the magnetic dipole allowed selection rule $\Delta m_I = \pm 1$, the resonance frequency is given by

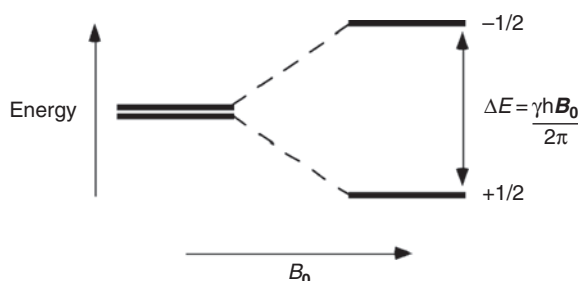


Figure 1.1. Energy levels for a nucleus with spin quantum number $I = \pm 1/2$. In the absence of an externally applied field, B_0 , the two energy levels are degenerate. Nuclei with spin 1/2 have two energy levels corresponding to the two discrete values of I . The spin with $I = +1/2$ is aligned with the external magnetic field and thus is lower in energy.

$$\nu_0 = \Delta E/\hbar = \gamma\hbar B_0/(2\pi\hbar) = \gamma B_0/2\pi \quad (1.4)$$

which can be expressed in angular frequency units (radians/sec) as

$$\omega_0 = \gamma B_0 \quad (1.5)$$

ω is called the Larmor frequency. With typical magnetic field strengths currently available for MRS in humans (≈ 1 to 7 Tesla), most magnetic nuclei resonate in the very high frequency (VHF) region of the electromagnetic spectrum (e.g. ≈ 42 –300 MHz for the protons). Magnets (1.5 and 3.0 T) are most commonly used for clinical MRS studies, corresponding to resonant frequencies of 64 and 128 MHz, respectively.

Signal and signal-to-noise ratio

In NMR, the difference between energy levels is very small and this results in very small population differences between the upper and lower energy levels. The excess population of the lower level compared to the upper level can be calculated from the Boltzmann factor

$$\frac{n(\text{upper})}{n(\text{lower})} = \exp(-\Delta E/kT) \quad (1.6)$$

where k is the Boltzmann constant (1.380650×10^{-23} J K $^{-1}$) and T is the absolute temperature (measured in Kelvin (K)). For protons at body temperature (310 K) at 128 MHz, $n(\text{upper})/n(\text{lower}) \approx 0.9999801$. The excess population of the lower level creates the macroscopic nuclear magnetization that is observed in the NMR experiment – note that this magnetization is very small, since, for instance in the example above, only 0.002% of the total number of spins contribute to the net nuclear magnetization, M_0 , which can be expressed as

$$M = NB_0\gamma^2\hbar^2 I(I+1)/3kT \quad (1.7)$$

N is the total number of spins in the sample, and \hbar is Planck’s constant divided by 2π . The signal (S) detected in the receiver coil is proportional to the magnetization times the resonant frequency

$$S \propto M_0\omega_0 = NB_0^2\gamma^3\hbar^2 I(I+1)/3kT \quad (1.8)$$

giving a final dependence of the signal on B_0^2 for a given nuclei (γ fixed), or alternatively a γ^3 dependence for different nuclei at a fixed B_0 . Notice also that the signal increases with decreasing temperature. Therefore, the best signal is obtained at high fields, from

high γ nuclei, and at low temperature. While the temperature and nuclei to be observed are often fixed for in vivo experiments, it is clear that the use of high magnetic fields results in larger signals.

In an NMR experiment, the ability to detect a signal depends not only on the signal amplitude, but also on the amount of noise in the spectrum (i.e. the signal-to-noise ratio (SNR)). Noise voltages arise from the random, thermal motion of electrons in the radiofrequency (RF) coil used to detect the signal, and depend on the resistance of the coil (including any effects that the sample may have on the coil). Resistance typically increases with increasing RF frequency, with the exact dependence depending on both the coil and the sample properties. For biological samples (which have appreciable electrical conductivity), it is generally thought that the noise voltage increases approximately linearly with frequency, so that there is expected to be a linear increase in SNR with B_0 .

The rotating frame: simple pulse sequences for spectroscopy

The simplest NMR pulse sequence involves applying a radiofrequency pulse (B_1) for a short period of time (τ), followed by collection of the signal without any field gradients applied (the so-called “free induction decay”, or FID). The way this experiment is best understood is to use the “rotating frame” reference; in this frame, the B_0 field is taken to define the direction of the Z -axis, while the B_1 -field is static (so long as the applied RF frequency pulse is exactly on-resonance with the Larmor frequency) and defines either the X - or Y -axes. Initially, when the spin system is at equilibrium, all the magnetization is aligned along the Z -axis; application of the RF pulse results in the rotation of the Z -magnetization about the axis of the applied RF field at a nutation rate of γB_1 . At the end of the RF pulse (of length τ), the magnetization will have rotated through the angle (α , the “flip angle”)

$$\alpha = \gamma B_1 \tau \quad (1.9)$$

The RF receiver coil only detects magnetization in the XY plane, so the largest signal occurs (with long repetition times, TR) when all the magnetization is tipped from the Z -axis into the transverse plane – this is called a 90 degree pulse ($\alpha = 90^\circ$) (Figure 1.2A). In general, the signal amplitude will vary as $\sin(\alpha)$ for a single RF pulse.

In addition to detecting FIDs, much of MRI and in vivo MRS relies on the detection of signals from *spin*

echoes. Spin echoes, first discovered by Erwin Hahn in 1950, [5] are signals that occur after the application of two or more RF pulses. Echoes generally can occur with pulses of any flip angle, but are conceptually easiest to understand when considering the 90° – 180° echo sequence first introduced by Carr and Purcell in 1954.[6] After the initial 90° pulse, spins precess around the Z -axis at a rate determined by the strength of the main magnetic field B_0 . Since the B_0 field is never completely uniform (homogeneous) throughout the different parts of the sample, different regions of the sample precess at different speeds, leading to a loss of phase-coherence between regions, and the loss of signal. By applying an 180° pulse at time $TE/2$ (where TE is echo time), the positions of the slow and fast precessing components are alternated in the transverse plane, and after another period of time $TE/2$ the magnetization vectors from all parts of the sample are in-phase again, leading to the creation of the echo signal (Figure 1.2B). If additional RF pulses are applied, additional echoes are formed. Commonly used pulse sequences for localized spectroscopy (see Chapter 2 for details) employ 3 pulses, such as a 90° – 180° – 180° (called the “PRESS” sequence), or 90° – 90° – 90° (called the “STEAM” sequence).

Relaxation times

After an RF pulse, the magnetization is tipped away from its equilibrium position aligned along the Z -axis of the rotating frame, and as a result it will start recovering back to its equilibrium position. The time-constant for this process (recovery of longitudinal magnetization) is known as the spin–lattice relaxation time constant, or T_1 . T_1 is usually measured using pulse sequences known as inversion-recovery (180° – TI – 90°) or saturation recovery (90° – TI – 90°), where the experiment is repeated with several different TI delay times in order to map out the signal vs. time curve (Figure 1.3). For the inversion recovery experiment, this curve takes the form $S(TI) = S(0)(1 - 2^* \exp(-TI/T_1))$, while for saturation recovery it becomes $S(TI) = S(0)(1 - \exp(-TI/T_1))$. Note that it is important to wait a sufficiently long repetition (TR , typically $> 5^*T_1$) between experiments for magnetization to fully recover before the next measurement or time average.

In addition to T_1 relaxation times, there is an additional time constant (T_2 , the transverse relaxation time) which describes how fast the transverse magnetization decays in a spin–echo experiment. The signal decay is

Chapter 1: Introduction to MR spectroscopy in vivo

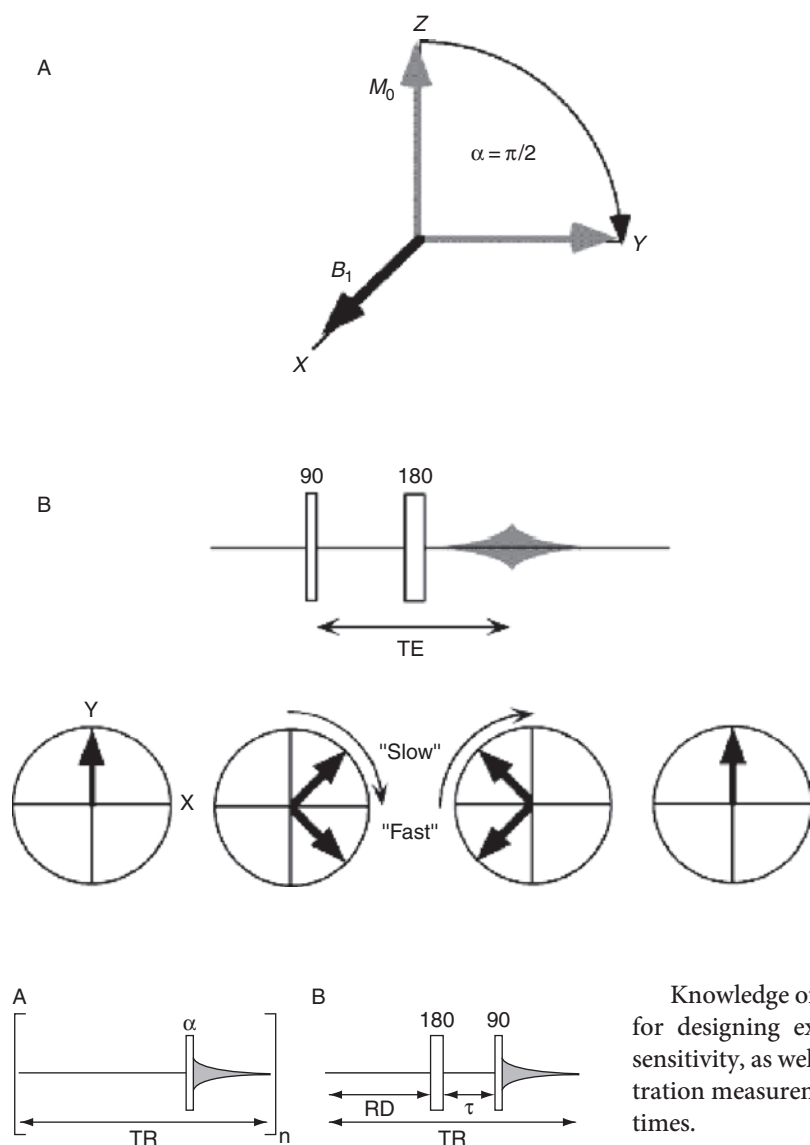


Figure 1.3. (A) Saturation and (B) inversion recovery experiments for the measurement of T_1 relaxation times. (A) The simplest pulsed experiment consists of a single RF pulse of flip angle, α , followed by detection of the FID, and can be repeated n times to improve the signal-to-noise ratio. (B) Diagram of the inversion recovery experiment that can be used to determine the T_1 relaxation time by varying the delay, τ , provided the recovery delay, RD , is $\sim 5 > T_1$.

described by the expression $SE(TE) = S(0)\exp(-TE/T_2)$, so T_2 is estimated from measurements of S performed as a function of TE . This can be done by repeating the measurement several times with different TE values (Carr–Purcell “Method A”) or by performing a single-shot multi-spin-echo experiment (i.e. multiple refocusing 180° pulses played out in a single experiment – Carr–Purcell “Method B”) (Figure 1.4).

Figure 1.2. (A) Effects of a 90° pulse in the rotating frame coordinate system. (B) Formation of a spin-echo using a 90° – 180° –acquire sequence.

Knowledge of relaxation times in vivo is important for designing experimental parameters for optimal sensitivity, as well as for correcting metabolite concentration measurements for effects of variable relaxation times.

Chemical shifts

Early in the development of NMR, it was discovered that nuclei in different molecular environments resonated at slightly different frequencies.[7] The origin of this effect lies in the response of the molecule’s electrons to the applied magnetic field; in simple terms, a rotating current is induced which generates a small magnetic field that (usually) opposes the external field (a *diamagnetic* effect). The nucleus thereby experiences a smaller net field than that which is actually applied – the effective field at the nucleus, $B_{0\text{eff}}$ can be expressed in terms of a shielding parameter, σ ,

$$B_{0\text{eff}} = B_0(1 - \sigma) \quad (1.10)$$

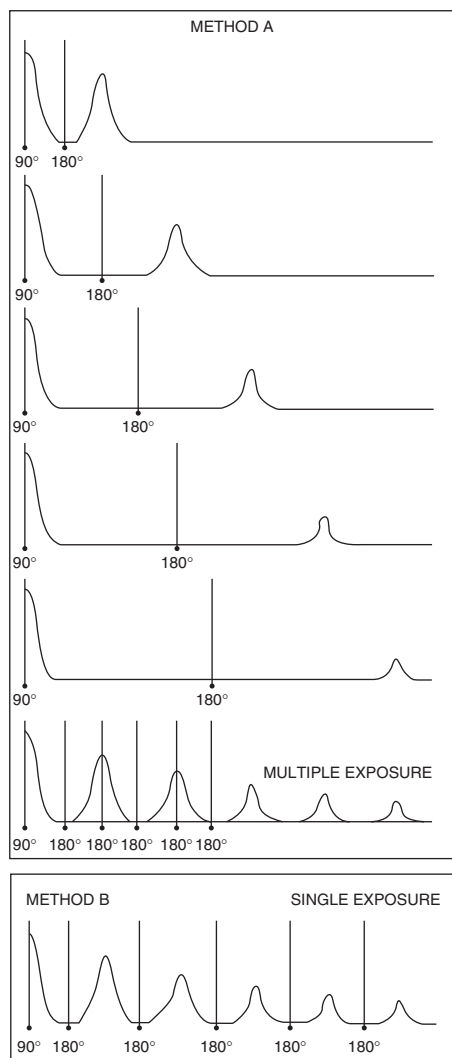


Figure 1.4. Measurement of T_2 relaxation times using either the Carr–Purcell Method “A” (a single 180° pulse) or Method “B” (multiple 180° pulses).

so that the nuclear resonance frequency becomes

$$\nu = \gamma B_{\text{eff}} / 2\pi = \nu_0(1 - \sigma) \quad (1.11)$$

This effect is known as the chemical shift; it is of prime importance, since nuclei in different chemical environments can be distinguished on the basis of their resonant frequencies. The shielding parameter is usually defined in parts per million (ppm) of the resonance frequency, measured relative to a reference compound. While the shielding parameter is a constant, the chemical shift (measured in Hz) increases linearly with field strength (Equation (1.10)). Thus the resolution of the NMR spectrum increases linearly

with increasing field strength, provided that the linewidths do not change. To compare chemical shifts measured at different field strengths, it is standard to report chemical shift values (δ) in ppm relative to a standard reference compound; for ^1H and ^{13}C spectra (in vitro), tetramethylsilane (TMS) is often used as the reference,

$$\delta = (\nu - \nu_{\text{ref}}) * 10^6 / \nu_{\text{ref}} \quad (1.12)$$

where ν and ν_{ref} are the frequencies of the signal of interest and the reference signal, respectively. In vivo, reference signals from compounds such as TMS are not available, so usually one of the indigenous spectral signals is used as a spectral reference (e.g. for ^1H spectra in the brain, the *N*-acetyl resonance of *N*-acetylaspartate (NAA), set to 2.02 ppm, is often used as a chemical shift reference).

Figure 1.5 illustrates the typical ^1H chemical shift range for various functional groups. While the typical chemical shift range for ^1H is quite small (≈ 10 ppm), much larger chemical shift ranges (e.g. up to several 100 ppm) exist for other nuclei such ^{19}F , ^{31}P , ^{13}C and ^{15}N .

Spin–spin (scalar) coupling constants

In addition to chemical shift effects, it was also discovered early in the development of NMR spectroscopy that spectra from liquid samples often exhibited further fine structure in the forms of splittings (or multiplets). [4] These arise from the electron-coupled spin–spin interaction, also known as J- or scalar-coupling. Spin–spin coupling results from nuclei experiencing the magnetic fields of their neighboring nuclei through polarization of the electrons in the molecular bonds between them. The effective magnetic field experienced by one nucleus depends on the spin state of a neighboring, coupled nucleus. The nomenclature to describe spin systems assigns letters to each individual spin, which are close together in the alphabet if the spins are strongly coupled or far from one another in the alphabet if the spins are weakly coupled ($|\delta_A - \delta_X| \gg J_{AX}$). The simplest multiplet pattern that can be observed is in a 2-spin, “AX” spin system (Figure 1.6).

Spin–spin couplings have the following properties:

1. They act through the bonding electrons and are therefore intramolecular.
2. They are independent of the strength of the applied magnetic field.
3. Spin multiplet structure reflects the states of neighbor nuclei.

Chapter 1: Introduction to MR spectroscopy in vivo

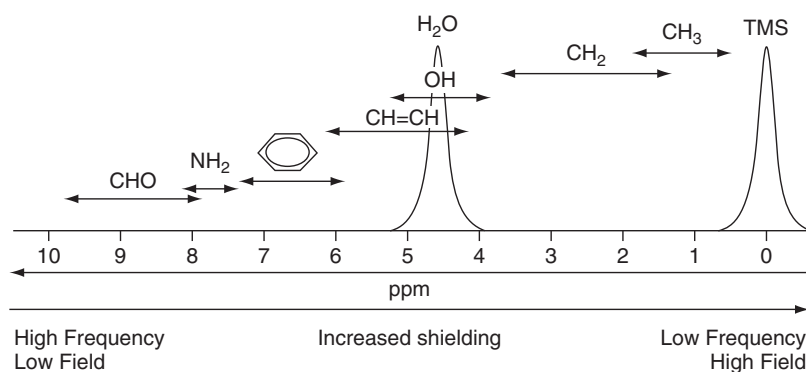


Figure 1.5. Typical ^1H chemical shift range (10 ppm) for various functional groups. The resonances of water and the standard reference compound TMS are shown at 4.7 and 0.0 ppm, respectively.

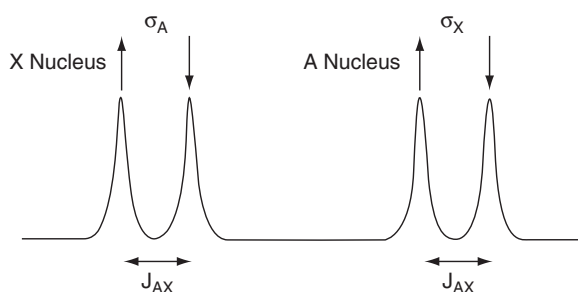


Figure 1.6. Multiplet pattern of a weakly coupled two-spin (AX) system. The splitting is equal to J_{AX} . σ represents the shielding constant of the A or X spin. The arrows indicate alignment with (\downarrow) or against (\uparrow) the static magnetic field.

- The interaction is reciprocal; if A splits X, then X splits A.
- Splitting cannot be observed due to coupling between equivalent nuclei.
- Coupling can be homonuclear or heteronuclear.

For spins which have widely different chemical shifts, the multiplet pattern is symmetrical around the chemical shift frequency, with relative intensities given by the binomial coefficients $(1+x)^N$ for $I = 1/2$ nuclei.

The simple treatment of multiplet patterns above is only valid if $|\delta_A - \delta_X| \gg J_{AX}$, which is known as the weak coupling, or first-order approximation. When this is not true, the spectra are strongly coupled or second-order, the symmetry of the multiplet is destroyed, and the splittings are no longer equal to the coupling constant. New lines may appear (combination lines), and lines are no longer assignable to a single nucleus. In general, the spectrum can only be assigned through the use of computer simulation. At the relatively low field strengths commonly used for in vivo MRS in humans, strong coupling is quite commonly encountered.

Nuclei with $I > 1/2$ produce more complicated multiplet patterns. The deuterium nucleus ($I = 1$) produces a triplet in neighboring atoms with an intensity ratio 1:1:1, corresponding to $m_I = -1, 0$ and $+1$, respectively. However, some quadrupolar nuclei relax too rapidly to generate observable splittings. It should also be noted that spin-spin splitting could be modified or eliminated by chemical exchange or double resonance experiments (decoupling).

Fourier transform spectroscopy

As mentioned above, virtually all MRS studies are performed by collecting time domain data after application of either a 90° pulse, or an echo-type of sequence. All resonances from the different molecules are collected simultaneously in the time domain, and the time domain signal (FID) is largely uninterpretable to the human eye. In order for a spectrum to be generated, it is necessary to perform Fourier transformation (FT), which allows the viewing of the signal intensity as a function of frequency (i.e. in the frequency domain) (Figure 1.7). Various filtering and other manipulations are often performed on the data both before and after fast Fourier transformation (FFT), which may have quite profound effects on the quality of the final spectrum; these are discussed in more detail in Chapter 3.

One advantage of pulsed FT is that all signals are being recorded at once, so it has a sensitivity advantage over alternative acquisition methods (“continuous-wave”, or CW), which recorded each part of the spectrum separately. In order to accumulate sufficient SNR with the pulsed FT method, the scan can be repeated many (N) times and averaged together (“time-averaging”) to improve SNR ($\propto \sqrt{N}$). The scan time will be $N \cdot TR$; it is important to choose the correct TR and the flip angle for optimum SNR. The seminal

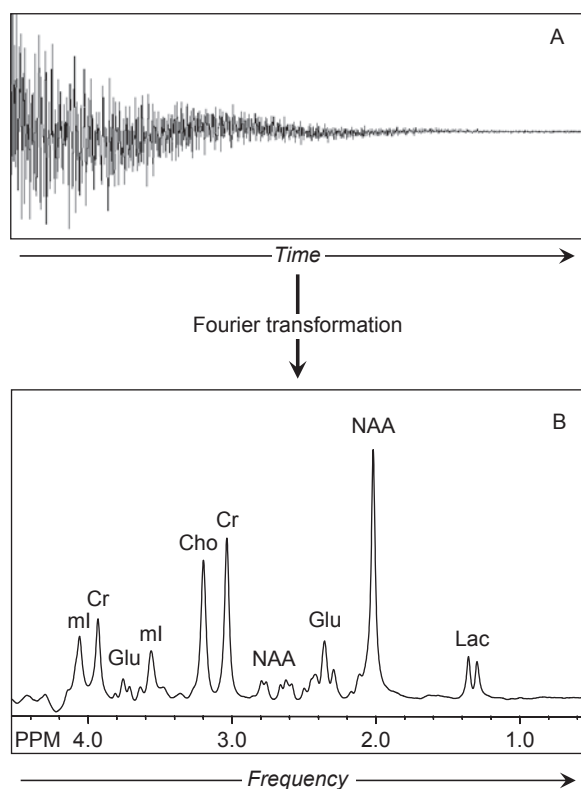


Figure 1.7. (A) An example of a free induction decay (FID, recorded as a function of time) and (B) the corresponding frequency domain spectrum obtained by Fourier transformation. The sample is a phantom containing *N*-acetyl aspartate (NAA, 2.01 and 2.6 ppm), creatine (Cr, 3.02 and 3.91 ppm), choline (Cho, 3.21 ppm), *myo*-inositol (ml, 3.56 and 4.05 ppm), glutamate (Glu, 2.34 and 3.74 ppm), and lactate (Lac, 1.31 ppm (doublet)), recorded at 3T with an echo time of 30 msec.

work by Ernst indicates that for optimum SNR the minimum TR should be chosen consistent with the pulse sequence being used and the desired spectral resolution (in Hz, equal to the inverse of the data readout window (acquisition time)), and then the flip angle set (the “Ernst Angle”) according to the expression, $\alpha = \cos^{-1}(\exp(-TR/T_1))$. For example, if $TR = 1.5$ sec and $T_1 = 1$ sec, $\alpha = 77.15^\circ$. [8,9]

In vivo MR spectroscopy

In vivo magnetic resonance spectroscopy (MRS) of the brain was first reported in the late 1970s in animal models. [10] Previous studies of biological tissues by NMR spectroscopy had focused on isolated, perfused organ systems or cell suspensions, and had indicated the feasibility of obtaining biochemical information non-invasively using NMR. Most of these studies used

the phosphorus-31 nucleus (^{31}P), since there was interest in measuring metabolism relating to bioenergetics, which involved compounds such as adenosine triphosphate (ATP), phosphocreatine (PCr) and inorganic phosphate (Pi). ^{31}P spectroscopy was relatively straightforward to perform, since the ^{31}P nucleus is spin-1/2 and has a reasonably high gyromagnetic (γ) ratio and chemical shift range (~ 40 ppm), and does not require any water suppression. It was also found that the resonance frequency of Pi was sensitive to pH, [11] and could be used to determine brain pH non-invasively, [12, 13] As interest in in vivo MRS and MRI increased, larger bore horizontal superconducting magnet systems were developed for this purpose, for larger animals and humans, although at lower field strengths than used for high-resolution NMR (e.g. 1.5–2.0 Tesla (T), 64–85 MHz for ^1H). An important technical advance was the introduction of local, surface RF coils that had high sensitivity, [14] and also limited signal reception to only tissues that are proximal to the coil, thereby eliminating signal from unwanted regions or other organs. These advances enabled the first observation of in vivo MRS in humans, [15] and the detection of birth asphyxia in the brain of infants, [16] using ^{31}P MRS. In addition to ^{31}P , there was also interest in the carbon-13 (^{13}C) nucleus, which, like ^{31}P , has some technical advantages, such as a wide chemical shift range (~ 200 ppm), spin-1/2, and no need for solvent suppression. [17] However, both ^{31}P , and ^{13}C suffer from relatively low sensitivity. In the case of ^{13}C , sensitivity is very low because of its low natural abundance (1%), although exogenously introduced isotopic enrichment can be used, which is in fact an important method for studying kinetics of metabolism. [17]

It was recognized that proton (^1H) spectroscopy would offer a large sensitivity advantage over these other nuclei, because the proton has the highest gyromagnetic ratio γ of non-radioactive nuclei, as well as a high natural abundance. Sensitivity is also enhanced compared to other nuclei because of favorable metabolite relaxation times, and also because several important brain metabolites have resonances resulting from functional groups with multiple protons (methyl groups with three protons). In order for proton MRS to be successful, however, water suppression techniques had to be developed for in vivo MRS, so as to remove the much larger water signal (compared to the metabolite signals), and magnetic field homogeneity and field strengths had to be sufficient to allow one to resolve the smaller chemical

Chapter 1: Introduction to MR spectroscopy in vivo

shifts of protons (range ~ 10 ppm). In 1983, Behar *et al.* reported the first in vivo MRS of the brain,[18] in rats at 360 MHz (~ 8.5 T) using a surface RF coil and a continuous, pre-saturation pulse for water suppression. Resonances were assigned (by comparison with high-resolution NMR spectra of perchloric acid extracts of brain tissue) to phosphocholine (PCho), phosphocreatine (PCr), creatine (Cr), aspartate (Asp), glutamate (Glu), *N*-acetyl aspartate (NAA), γ -amino butyric acid (GABA), alanine (Ala) and lactate (Lac). It was also demonstrated in the same paper that induction of hypoxia (by lowering the inspired oxygen fraction from 25% to 4% for 15 min) caused an elevation of the brain lactate signal, which could be reversed by restoration of 25% oxygen. In 1984, the same group demonstrated that proton spectra, somewhat less well-resolved, could also be obtained at the more clinically relevant field strength of 1.9 T, and that the use of a spin-echo pulse sequence provided improved water suppression, and removed lipids and broad baseline components, all of which have relatively shorter transverse (T_2) relaxation times than the small molecular weight metabolites.[19]

In 1985, Bottomley *et al.* reported the first spatially localized human brain spectrum, at 1.5 T using a slice-selective spin-echo excitation technique, and frequency selective water suppression.[20] At an echo time of 80 ms, signals were observed from NAA, Asp, creatine and choline-containing (Cho) compounds, as well as from lipids and residual water. Although this paper demonstrated the feasibility of human brain spectroscopy in vivo on a 1.5 T MRI system, the spatial localization and spectral resolution were limited. Similar approaches were used by Luyten and den Hollander [21] and Hanstock *et al.*[22] to record spectra from the human brain, using a spin-echo depth pulse localization scheme and surface coil reception. Using a 2.1 T magnet, Hanstock *et al.* demonstrated well-resolved signals for choline, creatine, NAA, as well as a combined peak of GABA, glutamate (Glu) and glutamine (Gln), which could be recorded from an approximate volume of 14 ml in a 4-min scan time. T_2 values of Cr and NAA were also estimated to be in the range 140–530 ms (with Cr appreciably shorter than NAA), and it was further demonstrated that a normal human brain lactate concentration of the order of 0.5 mM may be detectable using modulation of the spin-echo by J-coupling (a TE of 150 ms was used[22]).

However, spatial localization provided by depth pulses and surface coils is relatively ill-defined, and

therefore improved spatial localization techniques (in particular, definition of localization in all three dimensions) were required. Spatial localization allows signals to be recorded from well-defined structures or lesions within the brain, and by recording signals from smaller volume elements, improved field homogeneity can be obtained.[23] In the 1980s, a wide range of spatial localization techniques were developed for in vivo spectroscopy;[24] however, many were either difficult to implement, involved too many RF pulses, or were inefficient (i.e. involved too much signal loss, or did not fully suppress out-of-voxel magnetization). Out of this plethora of sequences, two emerged as simple and robust enough for routine use, each based on three slice-selective pulses applied in orthogonal directions. The STEAM sequence (Stimulated Echo Acquisition Mode)[25,26,27, 28] uses three 90° pulses and detects the resulting stimulated echo from the volume intersected by all three pulses, while the PRESS sequence uses one 90° pulse and two 180° pulses to detect a spin echo from the localized volume.[29,30] A detailed description of these techniques is provided in the next chapter. The demonstration in 1989 of high-resolution human proton brain spectra from relatively small, well-defined regions of interest in short scan times (generally less than 5 min) led to a rapid increase in the use of this methodology, and allowed for the non-invasive study of human brain metabolism in neuropathology by proton MRS in the early 1990s.[28]

Commercial availability and automation[31] of proton MRS on clinical MRI systems expedited these studies, as well as the transition of this method to the clinical examination. While human brain MRS in the 1980s was mainly focused on ^{31}P MRS,[32] the realization of the higher signal-to-noise ratios available with ^1H MRS, and the consequent improvements in spatial resolution, led to the adoption of ^1H MRS at the expense of ^{31}P . ^1H MRS also has the highly significant advantage over all other nuclei that it uses exactly the same hardware (RF coils, amplifiers, preamplifiers, receivers, etc.) as used in conventional MRI, thereby allowing it to be performed on most commercial MRI scanners without significant hardware modifications. At 1.5 T, proton MRS can typically be performed on voxel volumes of the order of $1\text{--}8\text{ cm}^3$, while ^{31}P MRS usually requires voxel volumes greater than 30 cm^3 . Therefore, the clinical applications of ^{31}P MRS are limited in the brain, because of low spatial resolution and signal-to-noise ratios (SNR). As mentioned above, ^{13}C MRS in the brain has even lower sensitivity (and hence spatial resolution) than ^{31}P , and therefore has

also remained solely a research tool, rather than becoming a clinical technique for use in radiology.

The remainder of this handbook is focused on methods for proton MRS of the human brain, since this is the technique that is overwhelmingly used to study human brain metabolism at present. Proton MRS also shows promise for the evaluation of other organ systems, particularly the prostate and breast. [33,34] In general, MRS outside of the brain presents a number of additional technical challenges that make it much harder to perform than in the central nervous system. For this reason, there has been greater emphasis on CNS applications so far; however, in the future this may change. The last few chapters of the handbook deal with techniques and application of MRS in the body.

Nuclei for in vivo MRS

By far the most in vivo MRS studies have been performed using the proton (^1H) nucleus, because of several reasons; the proton has high sensitivity because of its high γ and high natural abundance, as well as quite favorable relaxation times and spin half. In addition, the proton is also the nucleus used for conventional MRI, so proton MRS can be performed usually with exactly the same hardware as is used for conventional MRI. However, there are other nuclei which can be used for in vivo MRS if appropriate RF coils, amplifiers, and electronics are available; some examples include carbon-13 (^{13}C), nitrogen-15 (^{15}N), or phosphorus-31 (^{31}P): generally, these have lower sensitivity and natural abundance, which results in longer scan times and lower spatial resolution (increased voxel size). The properties of these nuclei are listed in Table 1.1. Since clinical applications of these nuclei are

Table 1.1. Properties of nuclei for in vivo MRS.

Nucleus	Frequency (MHz @1.5 T)	Spin	Natural abundance (%)
Proton (^1H)	63.9	1/2	99.98
Phosphorus (^{31}P)	25.9	1/2	100.00
Sodium (^{23}Na)	16.9	3/2	100.00
Carbon (^{13}C)	16.1	1/2	1.10
Deuterium (^2D)	9.8	1	0.02
Nitrogen (^{15}N)	6.5	1/2	0.37
Oxygen (^{17}O)	8.7	5/2	0.04
Fluorine (^{19}F)	59.8	1/2	100.00
Lithium (^7Li)	24.9	3/2	92.50

not yet routinely available, the majority of this book will focus on the use of the proton nucleus for in vivo MRS. However, it should be mentioned that the use of these nuclei with hyperpolarization and/or isotropic enrichment can give large sensitivity increases, and are the subject of active research efforts at present (2008). If technical challenges and cost issues can be overcome, methods based on these nuclei may offer unprecedented opportunities to study dynamic metabolic processes in humans non-invasively.

Information content of proton MR spectra of the brain

Because of the relatively low sensitivity of in vivo MRS, in order for a compound to be detectable, generally its concentration must be in the millimolar range, and it must be a small, mobile molecule. Large and/or membrane-associated molecules are not usually detected, although they may exhibit broad resonances that contribute to the baseline of the spectrum.[35]

The information content of a proton brain spectrum depends on quite a few factors, such as the field strength used, echo time, and type of pulse sequence. At the commonly used 1.5 T field strength, at long echo times (e.g. 140 or 280 ms are often used; Figure 1.8) only signals from Cho, Cr, and NAA are observed in normal brain, while compounds such as lactate, alanine, or others may be detectable if their concentrations are elevated above normal levels due to pathological processes.[36,37,38] At short echo times (e.g. 35 ms or less) compounds with shorter T_2 relaxation times (or multiplet resonances which become dephased at longer echo times) also become detectable. These include resonances from glutamate, glutamine, and GABA, which are not resolved from each other at 1.5 T, *myo*-inositol, as well as lipids and macromolecular resonances (Figure 1.8). Spectral appearance at 3.0 T is generally similar to that at 1.5 T (Figures 1.8C and D), although the coupling patterns of the multiplet resonances are somewhat different. Most of the multiplets (e.g. Glu, Gln, mI, taurine) are strongly coupled at these field strengths, and Glu and Gln overlap slightly less at 3 T than at 1.5 T. As field strengths increase further, to 4.0 and 7.0 T, spectral resolution progressively increases (provided that magnetic field homogeneity can be maintained) and more compounds can be assigned with confidence, including separating *N*-acetyl aspartyl glutamate (NAAG) from NAA, separation of Glu from Gln, and the detection of up to 14 different compounds at short echo times at 7 T (Figure 1.8E).[39] A complete

Chapter 1: Introduction to MR spectroscopy in vivo

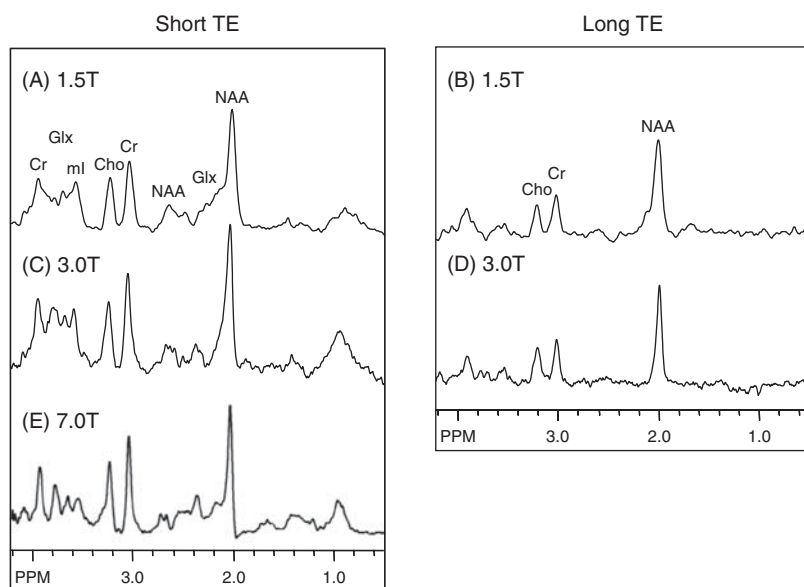


Figure 1.8. Single-voxel proton MRS of normal human brain white matter at different field strengths and echo times recorded using the STEAM pulse sequence ($2 \times 2 \times 2$ cm voxel size). 1.5T: (A) TE 20 ms, (B) TE 136 ms; 3.0T (C) TE 20 ms, (D) TE 136 ms; and 7.0T (E) TE 18 ms. Spectrum (E) provided by Dr James Murdoch, Philips Medical Systems. As field strength increases, spectral resolution improves, particularly for the strongly coupled resonances such as glutamate, glutamine, and myo-inositol.

list of metabolite structures, chemical shift, coupling constants, and multiplet patterns can be found in reference [40], and a summary of all compounds that have been detected in the human brain by proton MRS is given in Table 1.2.

NAA

The largest signal in the normal adult brain spectrum, the acetyl group of *N*-acetyl aspartate resonates at 2.01 ppm, with a usually unresolved (except at very high fields) contribution from *N*-acetyl aspartyl glutamate (NAAG) at 2.04 ppm.[41,42] The aspartyl group also exhibits a pH-sensitive, strongly coupled resonance at approximately 2.6 ppm. Despite being one of the most abundant amino acids in the central nervous system, NAA was not discovered until 1956, and its function has been the subject of considerable debate.[43] It has been speculated to be a source of acetyl groups for lipid synthesis, a regulator of protein synthesis, a storage form of acetyl-CoA or aspartate, a breakdown product of NAAG (which, unlike NAA, is a neurotransmitter), or an osmolyte.[44] NAA is believed to be synthesized in neuronal mitochondria, from aspartate and acetyl-CoA (Figure 1.9A). NAA is often referred to as a neuronal marker, based on several lines of evidence. For instance, immunocytochemical staining techniques have indicated that NAA is predominantly restricted to neurons, axons, and dendrites within the central nervous system;[45] and

studies of diseases known to involve neuronal and/or axonal loss (for instance, infarcts, brain tumors, or multiple sclerosis (MS) plaques) have without exception found NAA to be decreased. In pathologies such as MS, good correlations between brain NAA levels and clinical measures of disability have been found, suggesting that higher NAA levels may be associated with better neuronal function.[46] Animal models of chronic neuronal injury have also been shown to give good correlations between NAA levels (as measured by MRS) and in vitro measures of neuronal survival. [47] All of these studies therefore suggest that MRS measurements of NAA may be useful for assessment of neuronal health or integrity in the central nervous system.

However, other experiments suggest that caution should be used in interpreting NAA solely as a neuronal marker. For instance, it has also been reported that NAA may be found in non-neuronal cells, such as mast cells or isolated oligodendrocyte preparations, suggesting that NAA may not be specific for neuronal processes.[48,49,50] It is unclear if these cells are present at high enough concentrations in the normal human brain to contribute significantly to the NAA signal, however. There are also some rare cases where NAA metabolism is perturbed, almost certainly independently of neuronal density or function. One example is the leukodystrophy, Canavan's disease, which is associated with a large elevation of intracellular NAA, owing to deficiency of aspartoacylase, the enzyme that